



**Acoustics'08  
Paris**  
June 29-July 4, 2008

[www.acoustics08-paris.org](http://www.acoustics08-paris.org)

## Measurement of Sound Velocity in Water Using Optical Probe and Acoustical Holography

Takeshi Ohbuchi<sup>a</sup>, Koichi Mizutani<sup>b</sup>, Naoto Wakatsuki<sup>b</sup> and Hiroyuki Masuyama<sup>c</sup>

<sup>a</sup>University of Tsukuba, 1-1-1 Tennoudai, 305-8573 Tsukuba, Japan

<sup>b</sup>Tsukuba Univ., Tsukuba Science City, 305-8573 Ibaraki, Japan

<sup>c</sup>Toba National College of Maritime Technology, 1-1 Ikegami-cho, 517-8501 Toba, Japan  
ohbuchi@aclab.esys.tsukuba.ac.jp

We propose a method for determining a sound velocity in three-dimensional space with obstacles using a Michelson interferometer, optical computerized tomography (O-CT) and near-field acoustical holography (NAH). Ultrasonic waves affect the phase of a test light passing through the radiated sound fields. Zeroth-order diffraction light including sound pressure information is electrically acquired by an avalanche photodiode (APD). Projection data along the optical axis is obtained by single linear scanings in the range of  $\pm 20$  mm and electronically quadrature-detected as complex amplitude signal. Eighteen projections are acquired in the range of  $0 \leq \theta < \pi$  rad, and the complex sound fields are reconstructed in a region of  $28 \times 28$  mm<sup>2</sup> by O-CT. Then another plane separated by 5 mm is propagated using NAH from the acquired sound fields, and the same plane is reconstructed. Comparing the phase of the reconstructed and propagated sound fields in wave number domain, we determine the sound velocity in a region of  $28 \times 28 \times 5$  mm<sup>3</sup>. The experimental results are in agreement with a reference value.

## 1 Introduction

A temperature is an important parameter for system controls and quality controls. Currently, the major instrument for recording the temperature is a physical probe such as a thermocouple. However, the physical probe affects the temperature distribution and possesses a space. Then, an ultrasonic probe attracts attentions [1]. The ultrasonic probe obtains the temperature by measuring a sound velocity. Using the sound probe, only the mean temperature between two transducers is acquired. If the temperature distribution is acquired, computerized tomography (CT) [2] method is needed. This method, however, has a problem. The probe measuring the sound wave is on the sound beam axis. Thus, it is difficult to measure the sound velocity with obstacles on the sound beam axis.

For measuring the temperature with obstacles on the sound beam axis, we propose two methods. Firstly, to measure the sound wave, we use an optical probe [3]. To measure the sound wave with the optical probe, a refractive index fluctuation by the sound wave is utilized. The optical probe overcomes obstacles, because the optical probe is on the vertical axis of the sound beam. Secondly, to determine the sound velocity, we use near-field acoustical tomography (NAH) [4, 5]. A characteristic using NAH is that any sound source can be used. It is unnecessary that the sound wave is a plane wave.

In this paper, we propose the system for determining the sound velocity in a three-dimensional space with obstacles by measuring two two-dimensional sound fields using common sound source. The sound field is measured using Optical-CT method, and the sound velocity is determined using application of NAH.

## 2 Principle of measurement

### 2.1 Reconstruction of the sound fields

**Fig. 1** shows a schematic diagram of a Michelson interferometer and a light passing through the sound fields. The light source is a He-Ne Laser. The light is divided into two paths by a half mirror (HM). The propagating light, passing through a water tank containing the sound fields, is reflected by the reflecting mirror  $M_2$  and proceeds to HM.

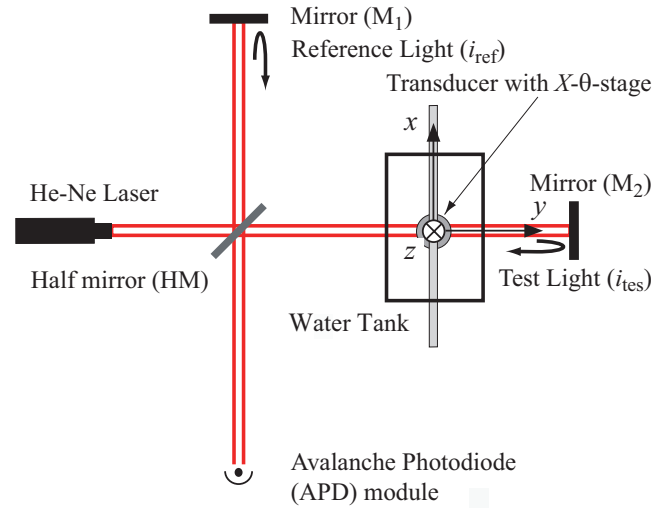


Fig.1 Schematic diagram of measuring system for sound field using Michelson interferometer.

This light is termed the “test light”. A phase of the test light is changed by changing a density of the medium. The other light is reflected by another mirror  $M_1$  and returned to HM. This is called the “reference light”. The test light and the reference lights are arranged in such a way that they may interfere with one another at an avalanche photo detector (APD). The optical intensity of the interference light  $I_{out}$  is given by

$$I_{out} = |i_{tes} + i_{ref}|^2 = I_{tes} + I_{ref} + 2\sqrt{I_{tes}I_{ref}} \cos \phi(x, t), \quad (1)$$

where the test light, the reference light and a phase difference between these lights are  $i_{tes}$ ,  $i_{ref}$  and  $\phi$ , respectively. Here, **Fig. 2** shows a geometry of coordinate system. A center of the transducer is an origin. The sound wave radiating for the  $z$  axis, and the light is radiating for the  $y$  axis. The plane of  $z=z$  is measured by the optical probe.

The optical intensities of the test light and the reference light are constant under a low sound pressure. Thus, the optical intensity of the interference light  $I_{out}$  is changed as the phase difference  $\phi$  and the phase difference changes by the sound wave. A relationship between amplitude of the sound pressure  $p_0$  and the phase difference  $\phi$  is expressed as

$$\phi(x, t) = \phi_c(x, t) + \phi_s(x, t) = \phi_c(x, t) + 2 \cdot \frac{2\pi\delta}{\lambda} \int p_0(x, y, t) dt, \quad (2)$$

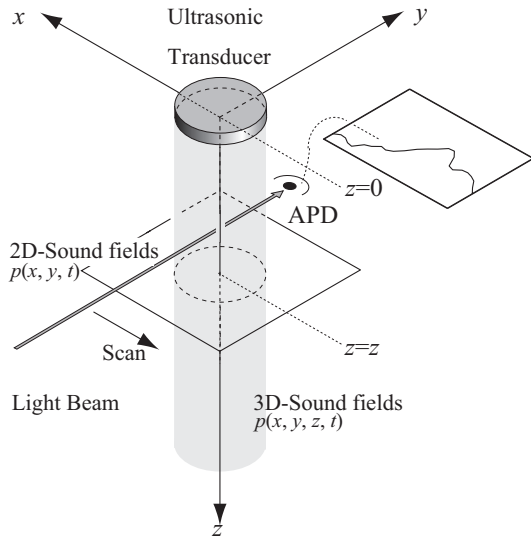


Fig.2 Geometry of coordinate system, ultrasonic transducer, sound field, reconstructed plane and propagated plane.

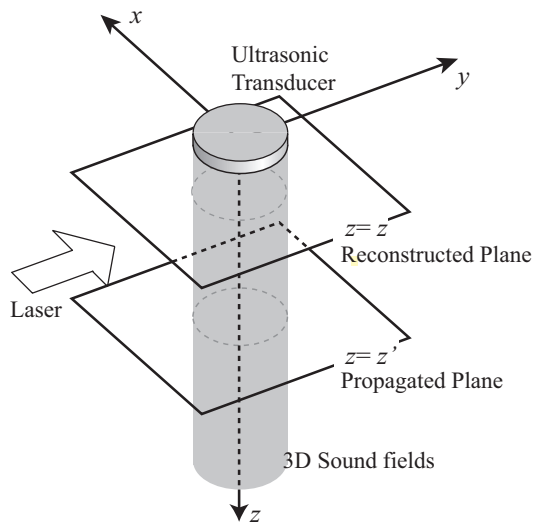


Fig.3 Geometry of coordinate system, ultrasonic transducer, sound field, reconstructed plane and propagated plane.

where  $\phi_c$ ,  $\phi_y$ ,  $\delta$  and  $\lambda$  are a phase difference under a static sound pressure, a phase difference by the sound pressure, a proportionality factor pertaining to the sound pressure and a refractive index [6] and a wavelength of the light, respectively.

The intensity of the interference light is detected by the APD, and a real part of the complex amplitude signal and an imaginary part of the complex amplitude signal are electrically obtained by a quadrature detector. The signals are projection data of the real and imaginary part of the complex sound pressure amplitude, respectively. Thus, some projections are obtained with rotation scannings, and the radiated sound field is reconstructed from projections using CT method [3].

## 2.2 Propagation of any sound field

The complex pressure of the sound fields given by the method described in above subsection at the plane of  $z=z$  are expressed as  $p_{CT}(x, y, z)$ . Any complex pressures at  $z=z'$

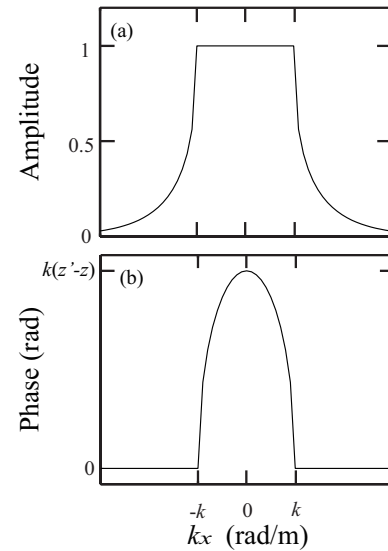


Fig.4 Frequency characteristic of propagation function. (a): amplitude of Frequency characteristic, (b):phase

expressed as  $p_{AH}(x, y, z')$  are propagated from the experimental data at the plane of  $z=z$  using NAH. Here, we consider a coordinate system as shown in Fig. 3. The propagated field is in parallel with the reconstructed field, and the ultrasonic transducer only vibrates along the  $z$ -axis.

A relationship between the complex sound pressure at the propagated field and at the reconstructed field is given by

$$p_{AH}(x, y, z') = p_{CT}(x, y, z) * h(x, y, z' - z), \quad (3)$$

where  $*$  and  $h$  denote convolution integral and a propagation function. When a spatial Fourier transform of the complex pressure of the sound fields and the propagation function are expressed as  $P_{CT}(k_x, k_y, z)$  and  $H(k_x, k_y, z' - z)$ , eq. (3) is transformed to

$$P_{AH}(k_x, k_y, z') = P_{CT}(k_x, k_y, z)H(k_x, k_y, z' - z). \quad (4)$$

Then, the complex sound pressure at the propagated field is propagated by computing a inverse Fourier transform of  $P_{AH}(k_x, k_y, z')$ , obtained by eq. (4). Here, the Fourier transform of the propagation function is given by a problem of a sound radiation from oscillating a flat plate, and expressed as

$$H(k_x, k_y, z' - z) = \exp\{ik_z(z' - z)\}, \quad (5)$$

$$k_z = \sqrt{k^2 - k_x^2 - k_y^2},$$

where  $k$  is a wavenumber [4]. Fig. 4 shows a frequency characteristic of the propagation function. The characteristic is changed at the wavenumber. Using the propagation function, any sound field can be propagated by the reconstructed sound field [5]. In addition, any sound sources are adequate, as far as we know that the phase of the ultrasonic wave is increased or decreased.

## 2.3 Determination of sound velocity

The wave number in water used for the propagation is determined by a water temperature and a frequency of the ultrasonic waves. Then, the actual wave number  $k_{CT}$  is determined by the propagated sound field using NAH at  $z=z'$  and the reconstructed sound field using CT at  $z=z$ .

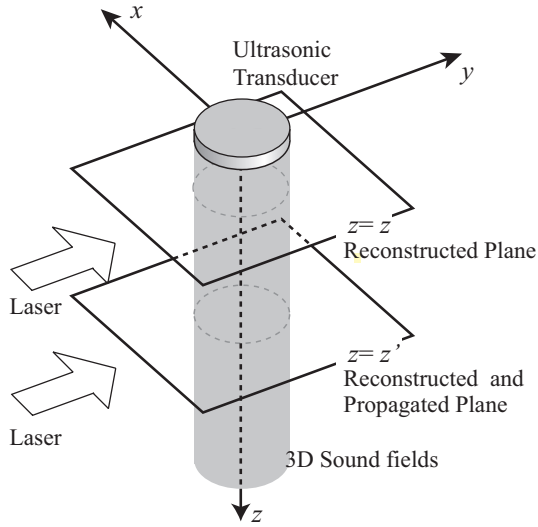


Fig.5 Geometry of coordinate system, ultrasonic transducer, sound field, reconstructed plane and propagated plane for measuring a sound velocity.

Fig.5 shows the coordinate system. Relational expressions of an assumed propagation function and the actual propagation function are given by

$$\begin{aligned} P_{AH}(k_x, k_y, z') &= P_{CT}(k_x, k_y, z) H_{AH}(k_x, k_y, z' - z), \\ P_{CT}(k_x, k_y, z') &= P_{CT}(k_x, k_y, z) H_{CT}(k_x, k_y, z' - z), \end{aligned} \quad (6)$$

where  $P_{AH}$ ,  $P_{CT}$ ,  $H_{AH}$  and  $H_{CT}$  are respectively a Fourier transform of the propagated sound pressure, of the reconstructed sound pressure, of the assumed propagation function, and of the actual propagation function. A phase difference between two reconstructed fields at  $z=z$  and  $z=z'$  is not suitable for a determination of the sound velocity, because the phase difference can be greater than  $2\pi$  at a close propagated distance. A phase difference between  $P_{CT}$  and  $P_{AH}$  is denoted  $\Phi_d$ , and the actual wave number  $k_{CT}$  is given by the phase difference.

$$\begin{aligned} \Phi_d &= (k_{zAH} - k_{zCT})(z' - z), \\ k_{zAH} &= \sqrt{k_{AH}^2 - k_x^2 - k_y^2}, \\ k_{zCT} &= \sqrt{k_{CT}^2 - k_x^2 - k_y^2}. \end{aligned} \quad (7)$$

Transforming eq. (7),

$$k_{CT} = \sqrt{\left| \frac{\Phi_d}{(z' - z)} - k_{zAH} \right|^2 + k_x^2 + k_y^2}. \quad (8)$$

Here, eq. (8) is fulfilled as

$$k_{CT}^2 \geq k_x^2 + k_y^2. \quad (9)$$

The actual wave number is given in the two-dimensional wave number domains. Under an isotropic and a homogeneous medium, the wave number is constant everywhere. Thus, the sound velocity is also constant.

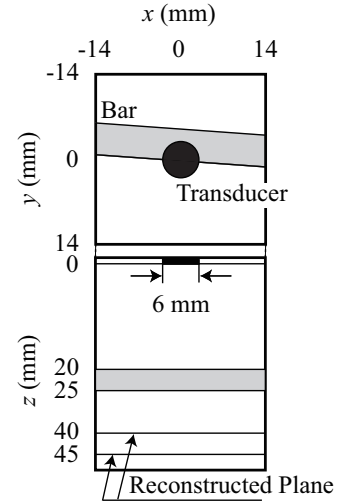


Fig.6 Geometry of coordinate system, ultrasonic transducer, metal bar, reconstructed plane and propagated plane.

### 3 Experimental Results

#### 3.1 Reconstruction of the sound fields

An experimental setup is shown in Fig. 1. A light source is a He-Ne laser (Melles Griot 05LHP151) with a light wavelength of 632.8 nm. The laser is branched into two light paths using a half mirror. An ultrasonic wave radiated from a transducer (PANAMETRICS A310S-SU) is installed in the companion path of two light paths with a water tank. A diameter of the piezoelectric transducer is 6.0 mm. The transducer is set to mechanical  $x$ - and  $\theta$ -stages and is scanned relative to the light beam. An optical intensity of interference light is measured by an APD module (Hamamatsu Photonics C533-03 7L-748). A one-dimensional distribution of the optical intensity along the  $x$ -axis is acquired by moving the  $x$ -stage, and projection data for reconstructing the sound fields using CT is acquired by moving the  $\theta$ -stage. The signal applied to the ultrasonic transducer is generated using a function generator (Hewlett Packard 33120A) at a frequency of 5.0 MHz. Signals of the intensity of the interference light are digitized using a digital oscilloscope (Hewlett Packard 54645A). Measured data are acquired into a personal computer (PC) through a General Purpose Interface Bus (GP-IB).

Fig. 6 shows a layout plan of the system for determining the sound velocity. In this paper, a metal bar is on the sound beam axis as an obstacle. A diameter of the bar is 5.0 mm, and the bar is at  $z=20$  mm. The bar is lean at an angle of 5 degree with the  $x$  axis. The reconstructed planes using CT are at  $z=40$  mm and  $z=45$  mm, and the reconstruction region in  $x$ - and  $y$ -directions are  $-14 \leq x \leq 14$  mm and  $-14 \leq y \leq 14$  mm, respectively.

The projection data for the CT are acquired by liner scan and rotation scan. The linear scanning region in the  $x$  direction is  $-20 \leq x \leq 20$  mm with 0.2 mm steps, and the range of the rotation is  $0 \leq \theta < \pi$  rad with  $\pi/18$  rad rotation step angles; 18 projection data are acquired.

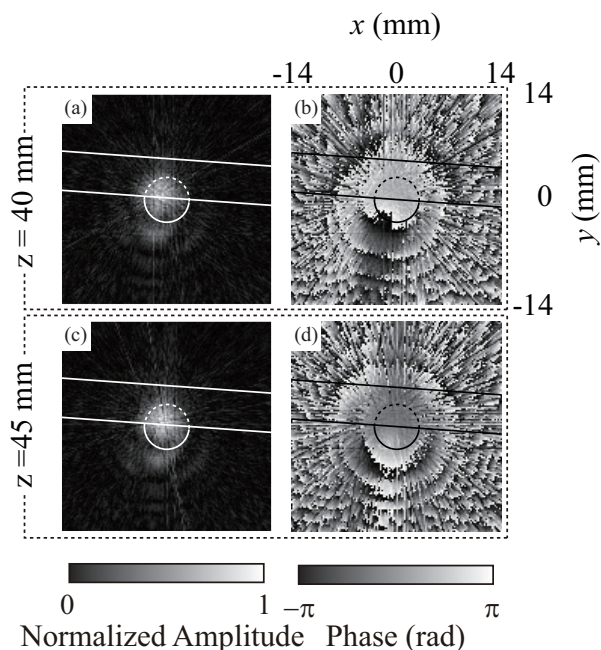


Fig.7 Experimental result of the reconstructed complex sound fields using CT. (a) and (b) the sound fields at  $z=40$  mm; (c) and (d) the sound fields at  $z=45$  mm. (a) and (c) the amplitude of sound fields; (b) and (d) the phase.

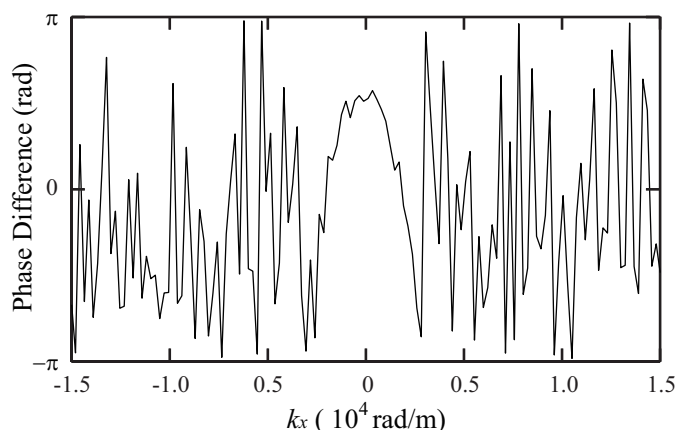


Fig.8 The phase difference in wavenumber domain between the reconstructed sound fields using CT and the propagated sound fields using NAH

**Fig. 7** shows a central parts of the reconstructed images, which denote the complex sound pressures at  $z=40$  mm and  $z=45$  mm. The reconstructed images of the sound fields at 40 mm from the vibrating surface are shown in Figs. 7(a) and 7(b), and the reconstructed images of the sound fields at 45 mm are shown in Figs. 7(c) and 7(d). Figs. 7(a) and 7(c) show amplitude images of the sound fields, and Figs. 7(a) and 7(c) show phase images of the sound fields. In Fig. 7, circles and parallel lines show the transducer and metal bar as the obstacle, respectively. The amplitude images shown in Fig. 7(a) and 7(c) have clear peak under the transducer, and the phase image shown in Fig. 7(b) and 7(d) have circular distributions as theoretical distributions. The images of the sound fields at  $z=40$  mm are similar to the images at  $z=45$  mm, and an influence by the obstacle is shown in Fig. 7. Using NAH, the sound fields at  $z=45$  mm is propagated by the sound fields at  $z=40$  mm.

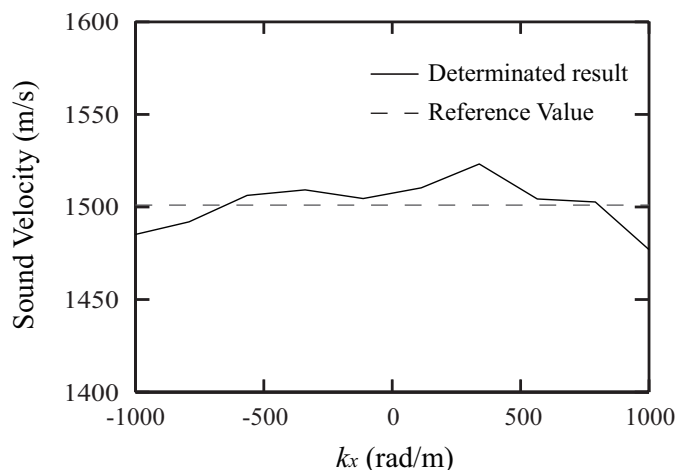


Fig.9 Profile of determined sound velocity in wave number domain. Solid line: determined result in the direction of  $k_x$ ; dashed line: reference value, sound velocity at 27 °C.

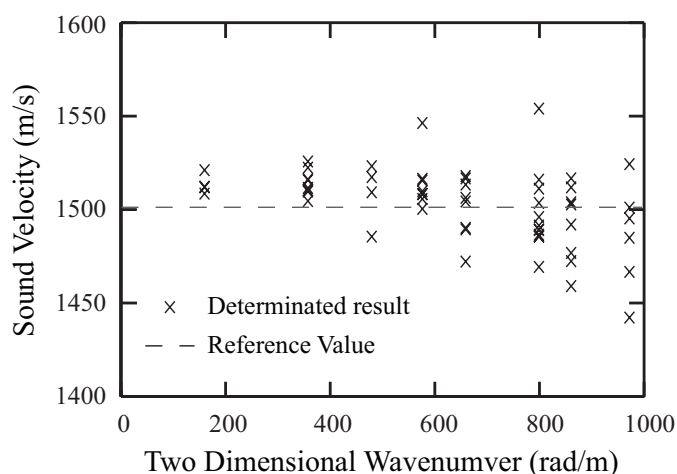


Fig.10 Determined sound velocity in wave number domain. dot 'x': determined result; dashed line; reference value, sound velocity at 27 °C.

**Fig. 8** shows a phase difference in a wavenumber domain between the reconstructed sound fields using CT and the propagated sound fields using NAH at  $z=45$  mm. Around range of  $-3000 \leq k_x \leq 3000$  rad/m, a peak is existed. The peak is similar to the phase of propagation function shown in Fig. 4. The results of reconstructed sound fields using CT are pertinent results to determine the sound velocity.

**Fig. 9** shows an experimental sound velocity profile in the wave number domain obtained using eq. (8). The solid line shows determined sound velocities in a direction of  $k_x$ , and the dashed line shows a reference value at 27 °C [7] of water, namely, 1501 m/s. The experimental sound velocity is around the reference value. However, the profile has outlier, caused by a fluctuation of the phase.

**Fig. 10** shows delaminated sound velocities in the two dimensional wavenumber domains. The result is spread. To determine the sound velocity, a median of the determined sound velocity in a range of  $k_{xy} \leq 1000$  rad/m is used. Where  $k_{xy}$  is a length of the two dimensional wavenumber vector. The median is 1508 m/s. The error is 7 m/s, and the error rate is about 0.53 %. These are good results for determining the sound velocity.

## 4 Conclusion

A constant sound velocity in a three-dimensional space with an obstacle was determined using O-CT and NAH. The sound fields radiated from a circular transducer with a diameter of 6.0 mm and driven at 5.0 MHz was reconstructed at a reconstructed plane, 40 mm from the transducer, and at a reconstructed and propagated plane, 45 mm from the transducer, using O-CT. A complex pressure at the reconstructed and propagated plane was propagated using NAH from the data reconstructed at the reconstructed plane.

The sound velocity was determined using the reconstructed and propagated sound fields at the propagated plane  $z=45$  mm. The determined sound velocity in a region of  $28 \times 28 \times 5 \text{ mm}^3$  was also in fair agreement with a sound velocity at  $27^\circ\text{C}$  in water. By improving the theory, we will be able to determine a distribution of a three-dimensional sound velocity.

The determination technique presented in this paper is expected to be applicable to the measurement of temperature and the detection of abnormality, among others.

## Acknowledgments

This work was supported by Grant-in-Aid for JSPS Fellows.

## References

- [1] Koichi Mizutani, Satoshi Kawabe, Ikumi Saito and Hiroyuki Masuyama, "Measurement of Temperature Distribution Using Acoustic Reflector Array", *Jpn. J. Appl. Phys.* 45, 4516-4520 (2006)
- [2] L. A. Shepp, B. F. Logan, "The Fourier reconstruction of a head section.", *IEEE Trans. Nucl. Sci.* NS21, 21-43, (1974)
- [3] Takeshi Obuchi, Hiroyuki Masuyama, Koichi Mizutani, Satoshi Nakanishi, "Optical Computerized Tomography for Visualization of Ultrasonic Fields Using Michelson Interferometer", *Jpn. J. Appl. Phys.* 45, 7152-7157 (2006)
- [4] Earl G. Williams and Henry D. Dardy, "Nearfield acoustical holography using an underwater, automated scanner", *J. Acoust. Soc. Am.* 78, 789-798 (1985)
- [5] Takeshi Ohbuchi, Koichi Mizutani, Naoto Wakatsuki, Hiroyuki Masuyama, Shingo Shibata, "Indirect Measurement of Vibrating Surface of Ultrasonic Transducer Using Optical Computerized Tomography and Acoustical Holography", *Jpn. J. Appl. Phys.* 46, 4629-4632 (2007)
- [6] K. L. Zankel, E. A. Hiedemann, "Diffraction of Light by Ultrasonic Waves Progressing with Finite but Moderate Amplitudes in Liquids", *J. Acoust. Soc. Am.* 31, 44-54 (1959)
- [7] V. A. Del Grosso, C. W. Mader, "Speed of Sound in Pure Water", *J. Acoust. Soc. Am.* 52, 1442-1446 (1972)